Eur. Phys. J. C (2018) 78:344
https://doi.org/10.1140/epjc/s10052-018-5817-x

THE EUROPEAN PHYSICAL JOURNAL C

Regular Article - Theoretical Physics

New feature of low p_T charm quark hadronization in pp collisions at $\sqrt{s} = 7$ TeV

Jun Song[1], **Hai-hong Li**[1,2], **Feng-lan Shao**[2,a]

[1] Department of Physics, Jining University, Jining 273155, Shandong, China
[2] School of Physics and Engineering, Qufu Normal University, Jining 273165, Shandong, China

Received: 12 February 2018 / Accepted: 16 April 2018 / Published online: 28 April 2018

Abstract Treating the light-flavor constituent quarks and antiquarks whose momentum information is extracted from the data of soft light-flavor hadrons in pp collisions at $\sqrt{s} = 7$ TeV as the underlying source of chromatically neutralizing the charm quarks of low transverse momenta (p_T), we show that the experimental data of p_T spectra of single-charm hadrons $D^{0,+}$, D^{*+} D_s^+, Λ_c^+ and Ξ_c^0 at mid-rapidity in the low p_T range ($2 \lesssim p_T \lesssim 7$ GeV/c) in pp collisions at $\sqrt{s} = 7$ TeV can be well understood by the equal-velocity combination of perturbatively created charm quarks and those light-flavor constituent quarks and antiquarks. This suggests a possible new scenario of low p_T charm quark hadronization, in contrast to the traditional fragmentation mechanism, in pp collisions at LHC energies. This is also another support for the exhibition of the soft constituent quark degrees of freedom for the small parton system created in pp collisions at LHC energies.

1 Introduction

The experimental study of the quark-gluon plasma (QGP), a new state of matter of QCD, is mainly through the heavy-ion collisions which can create the big thermal parton system with relatively long lifetime. Relative to heavy-ion collisions, proton-nucleus (pA) collisions create the "intermediate" parton system and proton-proton (pp) collisions create the "small" parton system. The deconfined medium is usually assumed to be not created in pA and pp collisions, at least up to RHIC energies. In particular, the data of pp collisions, in the context of heavy-ion physics, are usually served as the baseline to study the effects and/or properties of cold and hot nuclear matter in pA and AA collisions, respectively.

The Large Hadron Collider (LHC) pushes the center of mass energy per colliding nucleon up to TeV level, which brings new properties even for the small parton system created in pp collisions. Recent measurements in pp collisions at LHC energies from CMS and ALICE collaborations find several remarkable similarities with heavy-ion collisions. In high-multiplicity events of pp collisions, the phenomena such as long-range angular correlations [1,2] and collectivity [3,4], strangeness enhancement [5,6], and the increased baryon to meson ratio at low transverse momentum (p_T) [7–9] are observed. These phenomena were already observed in heavy-ion collisions at RHIC and LHC energies and are usually regarded as the typical behaviors related to the formation of QGP. Theoretical studies of these striking observations focus on what happens on the small parton system created in pp collisions at LHC energies through different phenomenological/theoretical methods such as the mini-QGP creation or phase transition [10–15], multiple parton interaction [16], string overlap and color re-connection at hadronization [17–20], etc.

In recent work [21], we found that the mid-rapidity data of p_T spectra of light-flavor hadrons in the low p_T range ($p_T \lesssim 6$ GeV/c) in pp collisions at $\sqrt{s} = 7$ TeV can be well understood by a phenomenological quark combination mechanism using the equal-velocity combination of up/down and strange quarks and antiquarks with constituent masses at hadronization. This suggests that the constituent quark degrees of freedom (CQdof) play an important role in low p_T hadron production in pp collisions at LHC energies, which indicates the possible existence of the underlying source with soft CQdof, a kind of new property for the small parton system created in pp collisions at LHC energies.

The hadronization of the charm quarks in pp collisions is usually described by the traditional fragmentation mechanism or fragmentation function. In this paper, we study

This work is supported by the National Natural Science Foundation of China under Grant Nos. 11575100, 11675091.

[a] e-mail: shaofl@mail.sdu.edu.cn

the possibility of a new phenomenological feature for the hadronization of low p_T charm quarks in pp collisions at LHC energies. As the aforementioned discussion, the production of light-flavor hadrons in pp collisions at LHC energies can be well described by the combination of light-flavor constituent quarks and antiquarks of low p_T. These constituent quarks and antiquarks also serve as an underlying source for the color neutralization of charm quarks at hadronization to form the single-charm hadrons. Specifically, the charm quark can pick up a co-moving light antiquark or two co-moving quarks to form a single-charm meson or baryon, where the momentum characteristic is the combination $p_H = p_c + p_{\bar{q},qq}$. This (re-)combination characteristic of charm quark hadronization will reflect in the momentum spectra of charm hadrons and, in particular, the ratio of charm baryon to charm meson. Therefore, in this paper, we apply a phenomenological quark (re-)combination mechanism (QCM) to study the mid-rapidity p_T spectra of single-charm mesons $D^{0,+}$, D^{*+}, D_s^+ and baryons Λ_c^+, Ξ_c^0 and the ratios among them, and compare our results with available experimental data and several theoretical predictions by fragmentation mechanism.

This paper is organized as follows: Sect. 2 will introduce a working model in quark (re-)combination mechanism for charm quark hadronization. Section 3 presents our results and relevant discussions. A summary is given finally in Sect. 4.

2 Charm quark hadronization in QCM

The (re-)combination mechanism of charm quark hadronization was proposed in the early 1980s [22–24] and has many applications in both hadron–hadron collisions [25–27] and relativistic heavy-ion collisions [28–31]. Because of the lack of the sufficient knowledge for the spatial information of the small parton system created in pp collisions at LHC energies, in this section, we present a working model for the (re-)combination hadronization of charm quarks in the low p_T range in momentum space, which only incorporates the most basic feature of QCM, i.e., the equal-velocity combination approximation. In the unclear non-perturbative dynamics issues such as the selection of different spin states and the formation competition between baryon and meson in the combination are treated as model parameters.

2.1 Formulas in momentum space

The momentum distributions of the single-charm meson $M_{c\bar{l}}$ and baryon $B_{cll'}$ in QCM, as formulated in e.g. [32,33] in general, can be obtained by

$$f_{M_{c\bar{l}}}(p) = \int dp_1 dp_2 f_{c\bar{l}}(p_1, p_2) \mathscr{R}_{M_{c\bar{l}}}(p_1, p_2; p), \qquad (1)$$

$$f_{B_{cll'}}(p) = \int dp_1 dp_2 dp_3 f_{cll'}(p_1, p_2, p_3) \mathscr{R}_{B_{cll'}}(p_1, p_2, p_3; p). \qquad (2)$$

Here, $f_{c\bar{l}}(p_1, p_2)$ is the joint momentum distribution for charm quark (c) and light antiquark ($\bar{l}$). $\mathscr{R}_{M_{c\bar{l}}}(p_1, p_2; p)$ is the combination function, that is, the probability density for the given $c\bar{l}$ with momenta p_1, p_2 combining into a meson $M_{c\bar{l}}$ with momentum p. It is similar for the baryon.

We take independent distributions for quarks of different flavors by neglecting correlations,

$$f_{c\bar{l}}(p_1, p_2) = f_c(p_1) f_{\bar{l}}(p_2), \qquad (3)$$

$$f_{cll'}(p_1, p_2, p_3) = f_c(p_1) f_l(p_2) f_{l'}(p_3). \qquad (4)$$

We suppose the combination takes place mainly for a quark and/or an antiquark taking a given fraction of momentum of the hadron so that the combination function is the product of Dirac delta functions,

$$\mathscr{R}_{M_{c\bar{l}}}(p_1, p_2; p) = \kappa_{M_{c\bar{l}}} \prod_{i=1}^{2} \delta(p_i - x_i p), \qquad (5)$$

$$\mathscr{R}_{B_{cll'}}(p_1, p_2, p_3; p) = \kappa_{B_{cll'}} \prod_{i=1}^{3} \delta(p_i - x_i p), \qquad (6)$$

where $\kappa_{M_{c\bar{l}}}$ and $\kappa_{B_{cll'}}$ are constants which are independent of the momentum but dependent on other ingredients such as the quark number so that all charm quarks can be correctly exhausted (after further including multi-charm hadrons).

Following our earlier work [21,34] for light-flavor hadrons in pp and p–Pb collisions at LHC energies, we adopt the co-moving approximation in combination, i.e., the charm quark combines with light quark(s) of the same velocity to form the charm hadron. Since the equal velocity implies $p_i = \gamma v m_i \propto m_i$, the momentum fraction is

$$x_i = m_i / \sum_j m_j, \qquad (7)$$

where the quark masses are taken to be the constituent masses. For light-flavor quarks, we take $m_u = m_d = 0.33$ GeV and $m_s = 0.5$ GeV, so that the data of momentum spectra of light-flavor hadrons are well explained [21,34]. The constituent mass of the charm quark is taken to have the usual value $m_c = 1.5$ GeV. We also consider m_c to have a larger value, 1.7 GeV, which can more suitably construct the masses of vector single-charm mesons and single-charm baryons in the ground state in the equal-velocity combination of the charm quark with light-flavor quarks. The resulting momentum spectra of single-charm hadrons only slightly broaden for the same charm quark spectrum $f_c(p)$. Therefore, we neglect the effect of the constituent mass uncertainty of the charm quark in this paper.

Substituting Eqs. (3)–(4) and (5)–(6) into Eqs. (1)–(2), we obtain the distributions of single-charm hadrons,

$$f_{M_{c\bar{l}}}(p) = \kappa_{M_{c\bar{l}}} f_c(x_1 p) f_{\bar{l}}(x_2 p), \tag{8}$$

$$f_{B_{cll'}}(p) = \kappa_{B_{cll'}} f_c(x_1 p) f_l(x_2 p) f_{l'}(x_3 p). \tag{9}$$

We rewrite the distribution functions of the charm hadrons,

$$f_{M_{c\bar{l}}}(p) = N_{M_{c\bar{l}}} f^{(n)}_{M_{c\bar{l}}}(p), \tag{10}$$

$$f_{B_{cll'}}(p) = N_{B_{cll'}} f^{(n)}_{B_{cll'}}(p), \tag{11}$$

where $f^{(n)}_{M_{c\bar{l}}}(p)$ is the normalized distribution function with $\int dp\, f^{(n)}_{M_{c\bar{l}}}(p) = 1$. $N_{M_{c\bar{l}}}$ is the momentum-integrated yield,

$$N_{M_{c\bar{l}}} = N_c N_{\bar{l}} \frac{\kappa_{M_{c\bar{l}}}}{A_{M_{c\bar{l}}}} = N_c N_{\bar{l}} \mathscr{R}_{c\bar{l}\to M_{c\bar{l}}}, \tag{12}$$

$$N_{B_{cll'}} = N_c N_l N_{l'} \frac{\kappa_{B_{cll'}}}{A_{B_{cll'}}} = N_c N_l N_{l'} \mathscr{R}_{cll'\to B_{cll'}}, \tag{13}$$

where the coefficient $A^{-1}_{M_{c\bar{l}}} = \int dp\, f^{(n)}_c(x_1 p)\, f^{(n)}_{\bar{l}}(x_2 p)$ and $A^{-1}_{B_{cll'}} = \int \mathrm{d}p \prod_{i=1}^{3} f^{(n)}_{q_i}(x_i p)$ with the normalized charm and light quark distribution $\int dp f^{(n)}_{c,l}(p) = 1$. We see that $\mathscr{R}_{c\bar{l}\to M_{c\bar{l}}} \equiv \kappa_{M_{c\bar{l}}}/A_{M_{c\bar{l}}}$ is nothing but the momentum-integrated combination probability of $c\bar{l} \to M_{c\bar{l}}$. It is similar for $\mathscr{R}_{cll'\to B_{cll'}} \equiv \kappa_{B_{cll'}}/A_{B_{cll'}}$.

$\mathscr{R}_{c\bar{l}\to M_{c\bar{l}}}$ and $\mathscr{R}_{cll'\to B_{cll'}}$ are parameterized. We use N_{M_c} to denote the total number of all single-charm mesons. $N_{c\bar{q}} = N_c\left(N_{\bar{u}} + N_{\bar{d}} + N_{\bar{s}}\right)$ is the possible number of all charm-light pairs. $N_{M_c}/N_{c\bar{q}}$ gives the flavor-averaged probability of a $c\bar{l}$ forming a charm meson. The average number of $M_{c\bar{l}}$ is $N_c N_{\bar{l}} \times \left(N_{M_c}/N_{c\bar{q}}\right) = P_{\bar{l}} N_{M_c}$ where $P_{\bar{l}} \equiv N_{\bar{l}}/N_{\bar{q}}$ denotes the probability of an antiquark with the flavor $\bar{l}$. For a given $c\bar{l}$ combination, it can form different J^P states, and we use $C_{M_{i,c\bar{l}}}$ to denote the probability of forming the particular spin state i and finally obtain the yield of the charm meson $M_{i,c\bar{l}}$,

$$N_{M_{i,c\bar{l}}} = C_{M_{i,c\bar{l}}} P_{\bar{l}} N_{M_c}. \tag{14}$$

In this paper we consider only the pseudo-scalar mesons $J^P = 0^-$(D^+, D^0 and D^+_s) and vector mesons $J^P = 1^-$ (D^{*+}, D^{*0} and D^{*+}_s) in the ground state. We introduce a parameter $R_{V/P}$ to denote the relative ratio of vector meson to pseudo-scalar meson of the same quark flavors, and we have

$$C_{M_{i,c\bar{l}}} = \begin{cases} \frac{1}{1+R_{V/P}} & \text{for } J^P = 0^- \text{ mesons},\\ \frac{R_{V/P}}{1+R_{V/P}} & \text{for } J^P = 1^- \text{ mesons}. \end{cases} \tag{15}$$

We take $R_{V/P} = 1.5$, the thermal weight value used in [33,35,36].

In the baryon sector, we have

$$N_{B_{i,cll'}} = C_{B_{i,cll'}} N_{iter,ll'} P_l P_{l'} N_{B_c}, \tag{16}$$

where N_{B_c} is the total number of all single-charm baryons, $N_{iter,ll'} P_l P_{l'}$ selects the particular flavor state ll', and $C_{B_{i,cll'}}$ selects the particular spin state. Here $P_l = N_l/N_q = N_l/(N_u + N_d + N_s)$ denotes the probability of a quark with the flavor l. $N_{iter,ll'}$ is the permutation number of ll' pair and is taken to be 1 for $l = l'$ and 2 for $l \neq l'$. We consider the production of the triplet (Λ^+_c, Ξ^+_c, Ξ^0_c) with $J^P = (1/2)^+$, the sextet (Σ^0_c, Σ^+_c, Σ^{++}_c, Ξ'^0_c, Ξ'^+_c, Ω^0_c) with $J^P = (1/2)^+$, and the sextet (Σ^{*0}_c, Σ^{*+}_c, Σ^{*++}_c, Ξ^{*0}_c, Ξ^{*+}_c, Ω^{*0}_c) with $J^P = (3/2)^+$, respectively, in the ground state. We introduce a parameter $R_{S1/T}$ to denote the relative ratio of $J^P = (1/2)^+$ sextet baryons to $J^P = (1/2)^+$ triplet baryons of the same quark flavors, and a parameter $R_{S3/S1}$ to denote that of $J^P = (3/2)^+$ sextet baryons to $J^P = (1/2)^+$ sextet baryons of the same quark flavors. We also take the effective thermal weight as a guideline [33] and take $R_{S1/T} = 0.5$ and $R_{S3/S1} = 1.5$, respectively. For $ll' = uu, dd, ss$,

$$C_{B_{i,cll'}} = \begin{cases} \frac{1}{1+R_{S3/S1}} & \text{for } \Sigma^{++}_c,\ \Sigma^0_c,\ \Omega^0_c,\\ \frac{R_{S3/S1}}{1+R_{S3/S1}} & \text{for } \Sigma^{*++}_c,\ \Sigma^{*0}_c,\ \Omega^{*0}_c. \end{cases} \tag{17}$$

For $ll' = ud, us, ds$,

$$C_{B_{i,cll'}} = \begin{cases} \frac{1}{1+R_{S1/T}(1+R_{S3/S1})} & \text{for } \Lambda^+_c,\ \Xi^0_c,\ \Xi^+_c\\ \frac{R_{S1/T}}{1+R_{S1/T}(1+R_{S3/S1})} & \text{for } \Sigma^+_c,\ \Xi'^0_c,\ \Xi'^+_c\\ \frac{R_{S1/T}R_{S3/S1}}{1+R_{S1/T}(1+R_{S3/S1})} & \text{for } \Sigma^{*+}_c,\ \Xi^{*0}_c,\ \Xi^{*+}_c. \end{cases} \tag{18}$$

We note that yields and momentum spectra of the final state Λ^+_c, Ξ^0_c and Ω^0_c after taking the decay contribution into account are not sensitive to the parameters $R_{S1/T}$ and $R_{S3/S1}$.

Considering that the single-charm mesons and baryons consume most of the charm quarks produced in collisions, we have the following approximated normalization to single-charm hadrons:

$$N_{M_c} + N_{B_c} \approx N_c. \tag{19}$$

Here we treat the ratio $R^{(c)}_{B/M} \equiv N_{B_c}/N_{M_c}$ as a parameter of the model, which characterizes the relative production of single-charm baryons to single-charm mesons. We take $R^{(c)}_{B/M} = 0.425$, the same as that at mid-rapidity in p–Pb collisions [33].

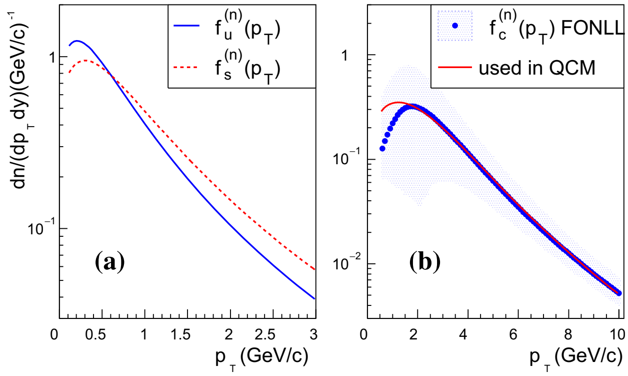

Fig. 1 **a** The normalized p_T spectra of light quarks at mid-rapidity in pp collisions at $\sqrt{s} = 7$ TeV; **b** that of charm quarks. The shadow area shows the scale uncertainties in FONLL calculation

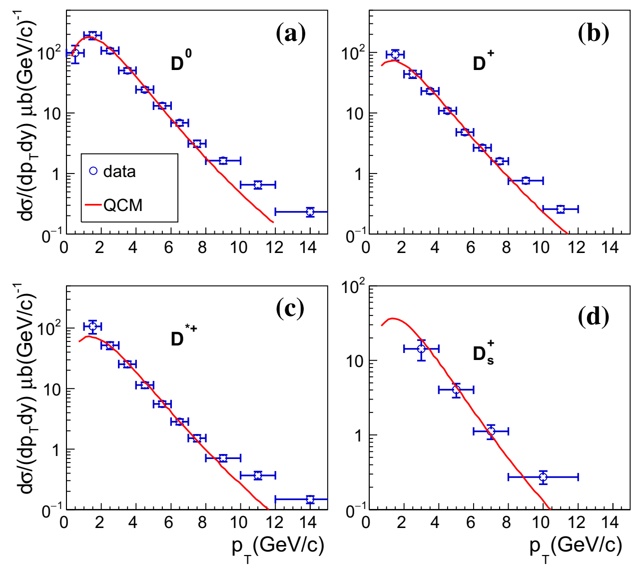

Fig. 2 Differential cross-sections of D mesons at mid-rapidity as the function of p_T in pp collisions at $\sqrt{s} = 7$ TeV. Symbols are experimental data [40] and lines are results of QCM

3 Results and discussions

We apply the above formulas in QCM to the one dimensional p_T space and calculate the p_T spectra of single-charm hadrons at mid-rapidity in pp collisions at $\sqrt{s} = 7$ TeV. The p_T distributions of quarks at hadronization are inputs of the model. We have obtained the p_T spectra of light-flavor constituent quarks in the previous work [21]. The averaged quark numbers in the rapidity interval $|y| < 0.5$ are 2.5 for the u quark and 0.8 for the s quark, respectively. The normalized distributions $f_u^{(n)}(p_T)$ and $f_s^{(n)}(p_T)$ are shown in Fig. 1a. The charge conjugation symmetry between quark and antiquark and the iso-spin symmetry between up and down quarks are applied in calculations.

In Fig. 1b, we show the normalized distribution of charm quarks, which is obtained from the online calculation of Fixed-Order Next-to-Leading-Logarithmic (FONLL). [1] The points are center values and the shadow area shows the scale uncertainties; see Refs. [37,38] for details. The uncertainty due to parton distribution functions (PDFs) is not included. Because of the large theoretical uncertainty, in particular, at low p_T, we only take the FONLL calculation as a guideline. The practically used p_T spectrum of charm quarks is reversely extracted from the data of D^{*+} meson [39,40] in QCM with charm quark constituent mass $m_c = 1.5$ GeV and is shown as the thick solid line in Fig. 1b. The cross-section of charm quarks in $|y| < 0.5$ interval is 1.2 mb. The extracted spectrum is found to be very close to the center values of FONLL calculation for $p_T \gtrsim 1.5$ GeV/c. We emphasize that just this good agreement prompts us to consider the QCM being the probable physical picture of low p_T charm quark hadronization. Whether this agreement is coincidental or not can be tested in the future by the data of higher collision energies, such as those in pp collisions at $\sqrt{s} = 13$ TeV.

In Fig. 2, we show results of differential cross-sections of D mesons at mid-rapidity as the function of p_T in pp collisions at $\sqrt{s} = 7$ TeV, and we compare them with experimental data [40]. We see that QCM well describes the data of D mesons for $p_T \lesssim 7$ GeV/c but under-predicts the data for larger p_T. This is reasonable. In the equal-velocity combination of charm quarks and light quarks, a charm quark with $p_{T,c} \lesssim 6$ GeV/c will combine a light antiquark of $p_{T,\bar{l}} \lesssim 1.5$ GeV/c. Because most of the light quarks, see Fig. 1a, are of such low p_T, they provide the sufficient partners (or chance) for the hadronization of charm quarks. For a charm quark of $p_{T,c} \gtrsim 6$ GeV/c, the combining light antiquark should have $p_{T,\bar{l}} \gtrsim 1.5$ GeV/c where the number density of light antiquark is very small and drops exponentially. In this case, those light antiquarks may be not enough to provide the sufficient chance for the combination hadronization of charm quarks of $p_{T,c} \gtrsim 6$ GeV/c, and therefore the combination may be not the dominated channel and the fragmentation will take over.

In Fig. 3, we show results for the ratios of different D mesons as a function of p_T in pp collisions at $\sqrt{s} = 7$ TeV, and we compare them with experimental data [40]. We see that, within experimental uncertainties, the model results are in agreement with the data. For the magnitudes of these four ratios, we can give a simple explanation from the yield (corresponding to differential cross-section) ratios of D mesons. Using Eq. (14) and taking strong and electromagnetic decay contribution into account where the data of decay branch ratios are taken from PDG[41], we have

$$\frac{D^+}{D^0} = \frac{1 + 0.323 R_{V/P}}{1 + 1.677 R_{V/P}} \approx 0.42, \tag{20}$$

[1] FONLL Heavy Quark Production, http://www.lpthe.jussieu.fr/~cacciari/fonll/fonllform.html.

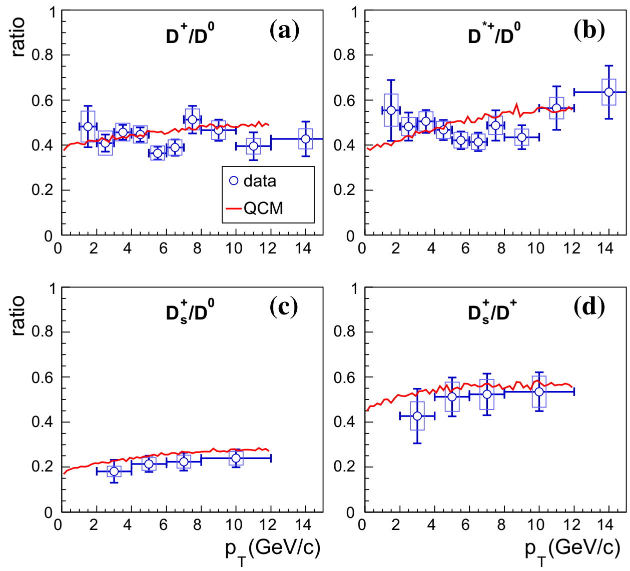

Fig. 3 Ratios of different D mesons as the function of p_T in pp collisions at $\sqrt{s} = 7$ TeV. Symbols are experimental data [40] and lines are results of QCM

$$\frac{D^{*+}}{D^0} = \frac{R_{V/P}}{1 + 1.677 R_{V/P}} \approx 0.43, \tag{21}$$

$$\frac{D_s^+}{D^0} = \frac{1 + R_{V/P}}{1 + 1.677 R_{V/P}} \lambda_s \approx 0.23, \tag{22}$$

$$\frac{D_s^+}{D^+} = \frac{1 + R_{V/P}}{1 + 0.323 R_{V/P}} \lambda_s \approx 0.54, \tag{23}$$

with $\lambda_s = N_s/N_u = 0.32$ and $R_{V/P} = 1.5$. Here, we emphasize that the value of $R_{V/P}$ is not specifically tuned to reproduce the data of these four ratios but is taken from the analysis of the effective thermal weight [42], which was often used in charm meson production [35,36].

Theoretical pQCD calculations with fragmentation functions were compared with experimental data of D mesons in Refs. [39,40]. It is shown that pQCD calculations in large p_T range have small theoretical uncertainties and often well explain the data. However, pQCD calculations in the small p_T range have quite large theoretical uncertainties and the comparison with data is not conclusive. In contrast with those pQCD calculations with fragmentation functions, our results suggest a different mechanism for the charm quark hadronization at low p_T.

The production of baryons is more sensitive to the hadronization mechanism. In Fig. 4, we show results of the p_T spectrum of baryon Λ_c^+ and the ratio to the D^0 meson, and we compare them with the experimental data [9]. We emphasize that, after taking the decay contribution of Σ_c and Σ_c^* into account, results of Λ_c^+ are not sensitive to model parameters $R_{S1/T}$ and $R_{S3/S1}$. We see that, similar to D mesons, our results of Λ_c^+ spectrum and ratio Λ_c^+/D^0 are

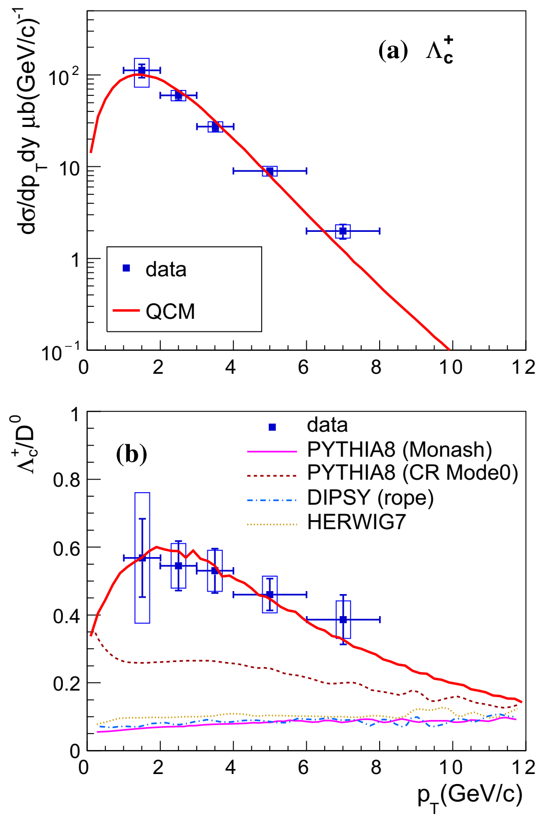

Fig. 4 Differential cross-section of Λ_c^+ at mid-rapidity (**a**) and the ratio to D^0 (**b**) as the function of p_T in pp collisions at $\sqrt{s} = 7$ TeV. Symbols are experimental data [9] and the thick solid lines are results of QCM. Results of other models or event generators in panel (**b**) are taken from [9]

in good agreement with the data for $p_T \lesssim 7$ GeV/c. The predictions of other models or event generators [20,43–45] which adopt string or cluster fragmentation mechanism for hadronization are also shown in Fig. 4b. PYTHIA8 Monash tune [46], DIPSY with rope parameter [43], and HERWIG7 [44] predict a small Λ_c^+/D^0 ratio of 0.1 and almost constant behavior at different p_T. Considering the effect of string formation beyond leading color approximation [20], PYTHIA8 (CR Mode0) increases the ratio to a certain extent and gives the decreasing tendency with p_T.

In Fig. 5, we show results of the differential cross-section of Ξ_c^0 at mid-rapidity multiplied by the branch ratio into $e^+\Xi^-\nu_e$ (a) and the relative ratio to D^0 (b) as the function of p_T in pp collisions at $\sqrt{s} = 7$ TeV. The decay contribution of Ξ_c' and Ξ_c^* is included, and results of Ξ_c^0 are not sensitive to model parameters $R_{S1/T}$ and $R_{S3/S1}$. Because of the lack of the absolute branch ratio into $e^+\Xi^-\nu_e$, our result of the spectrum of Ξ_c^0 is multiplied by a branch ratio 3.8%, which is within the current range of theoretical calculations (0.83–4.2%) [47–49]. We see that the model result, the thick solid line in Fig. 5a, can well describe the data of Ξ_c^0 for $2 \lesssim p_T \lesssim 7$ GeV/c but significantly underestimates the first data

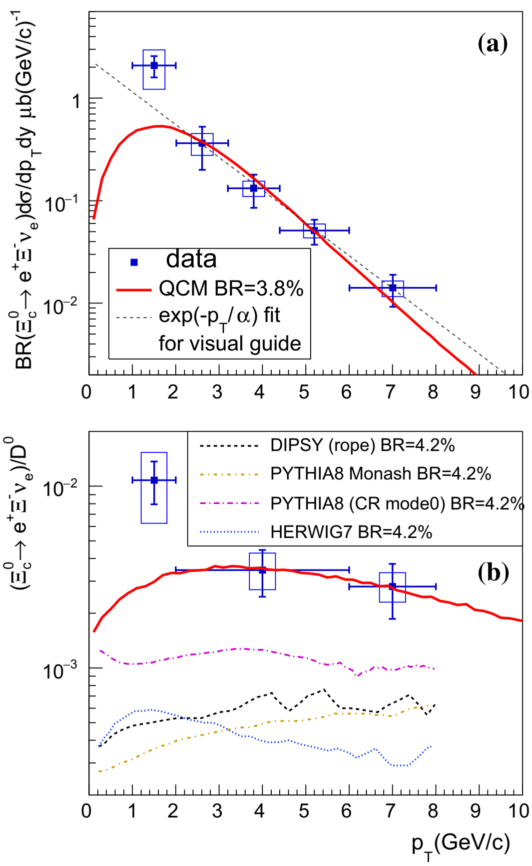

Fig. 5 Differential cross-section of Ξ_c^0 at mid-rapidity multiplied by the branch ratio into $e^+\Xi^-\nu_e$ (**a**) and the ratio to D^0 (**b**) as the function of p_T in pp collisions at $\sqrt{s}=7$ TeV. Symbols are experimental data [51] and the thick solid lines are results of QCM. Results of other models or event generators in panel (**b**) are taken from [51]

point at $p_T = 1.5$ GeV/c. However, the first data point, to our knowledge, is somewhat puzzlingly high if we note that the studied differential cross-section is $\mathrm{d}\sigma/\mathrm{d}p_T\mathrm{d}y$. The data of Λ_c^+ in Fig. 4a and D^0 in Fig. 2a suggest that the differential cross-section tends to increase slowly with the decreasing p_T for small $p_T \lesssim 2$ GeV/c and will saturate and decrease as $p_T \to 0$. The data of light-flavor hadrons for $\mathrm{d}N/\mathrm{d}p_T\mathrm{d}y$, e.g. K (892)*, show this behavior more clearly [50]. As a naive illustration, we see the first data point of Ξ_c^0 at $p_T = 1.5$ GeV/c is more than twice the exponential extrapolation from data points of larger p_T, the thin dashed line, which is not the case for the data of D mesons and Λ_c^+. The QCM result of the ratio Ξ_c^0/D^0 is shown in Fig. 5b. We see that the two data points within $2 \lesssim p_T \lesssim 7$ GeV/c can be well described by QCM and the first data point at $p_T = 1.5$ GeV/c is much higher than the QCM result.

String/cluster fragmentation usually under-predicts the production of Ξ_c^0. Here, we show predictions of several models or event generators which adopt string/cluster fragmentation at hadronization. They are taken from Ref. [51] and are shown as different kinds of thin lines in Fig. 5b. The decay branch $\Xi_c^0 \to e^+\Xi^-\nu_e$ is taken to be 4.2%, and therefore these predictions correspond to the up limits. HERWIG7 [44] which adopts the cluster fragmentation predicts the decreasing ratio for $p_T \gtrsim 1$ GeV/c but is lower than the data about an order of the magnitude. PYTHIA8 (Monash tune) [46] and DIPSY with rope parameter [43] which adopt sting fragmentation predict the increasing ratio as the function of p_T but the magnitude of the ratio is significantly lower than the data. PYTHIA8 (CR mode0) [20], which takes the color reconnection into account by considering the string formation beyond the leading color approximation, increases the prediction of ratio to a large extent but the prediction is still only one third of the data.

4 Summary and discussion

We have shown the experimental data of p_T spectra of single-charm hadrons $D^{0,+}$, D^{*+} D_s^+, Λ_c^+ and Ξ_c^0 at mid-rapidity in the low p_T range ($2 \lesssim p_T \lesssim 7$ GeV/c) in pp collisions at $\sqrt{s}=7$ TeV can be well understood by the equal-velocity combination of perturbatively created charm quarks and the light-flavor constituent quarks and antiquarks. We emphasize the following aspects to address the physical importance of our results: (1) The property, i.e., the p_T distributions, of light-flavor constituent quarks and antiquarks at hadronization is obtained from the data of p_T spectra of light-flavor hadrons in work [21] where it is found that equal-velocity combination of light-flavor quarks can reasonably describe the data of light-flavor hadrons in the low p_T range. The existence of the underlying source of light-flavor quarks is a new property of small parton system, maybe related to the creation of the deconfined parton system in pp collisions at LHC energies. (2) The good performance for the combination of charm quarks and those light-flavor quarks and antiquarks in comparison with the data suggests a new scenario of the low p_T charm quark hadronization in the presence of the underlying light quark source in pp collisions at LHC energies, in contrast to the usually adopted fragmentation mechanism. (3) Most of the light quarks combine into light-flavor hadrons that reproduces the data of light-flavor hadrons. A small fraction of light quarks combine with charm quarks, which also well explains the data of single-charm hadrons in low p_T range. This suggests a possible universal picture for the production of low p_T hadrons in pp collisions at LHC energies. Finally, such a new picture is also expected in the production of other heavy-flavor hadrons, and can be further tested in the future by the data of high spin charm hadrons as well as those of bottom hadrons.

Several discussions on the limitation of our model and results are necessary. The present work only focuses on the characteristic of hadron production in (transverse) momentum space. It is still unclear that what kind of the spatial property for the (light-flavor dominated) small parton system leads to the effective combination of charm quarks and those light-flavor quarks. In particular, in the light-flavor sector we adopt the concept of the constituent quarks. What kind of the spatial property for the small parton system is responsible for the exhibition of the soft light-flavor constituent quarks degrees of freedom? Is it related to the possible de-confinement in the small system of *pp* collisions at LHC energies? These interesting and important questions are deserving of study in the future.

Acknowledgements We thank Gang Li, Zuo-tang Liang, Wei Wang, and Rui-qin Wang for helpful discussions.

References

1. V. Khachatryan et al., JHEP **09**, 091 (2010). https://doi.org/10.1007/JHEP09(2010)091. arXiv:1009.4122 [hep-ex]
2. V. Khachatryan et al., Phys. Rev. Lett. **116**(17), 172302 (2016). https://doi.org/10.1103/PhysRevLett.116.172302. arXiv:1510.03068 [nucl-ex]
3. V. Khachatryan et al., Phys. Lett. B **765**, 193 (2017). https://doi.org/10.1016/j.physletb.2016.12.009. arXiv:1606.06198 [nucl-ex]
4. A. Ortiz Velasquez, Nucl. Phys. A **932**, 146 (2014). https://doi.org/10.1016/j.nuclphysa.2014.07.034. arXiv:1404.4354 [hep-ex]
5. J. Adam et al., Phys. Lett. B **758**, 389 (2016). https://doi.org/10.1016/j.physletb.2016.05.027. arXiv:1512.07227 [nucl-ex]
6. J. Adam et al., Nat. Phys. **13**, 535 (2017). https://doi.org/10.1038/nphys4111. arXiv:1606.07424 [nucl-ex]
7. B.B. Abelev et al., Phys. Lett. B **728**, 25 (2014). https://doi.org/10.1016/j.physletb.2013.11.020. arXiv:1307.6796 [nucl-ex]
8. J. Adam et al., Phys. Lett. B **760**, 720 (2016). https://doi.org/10.1016/j.physletb.2016.07.050. arXiv:1601.03658 [nucl-ex]
9. S. Acharya, et al., (2017). arXiv:1712.09581 [nucl-ex]
10. F.M. Liu, K. Werner, Phys. Rev. Lett. **106**, 242301 (2011). https://doi.org/10.1103/PhysRevLett.106.242301. arXiv:1102.1052 [hep-ph]
11. K. Werner, I. Karpenko, T. Pierog, Phys. Rev. Lett. **106**, 122004 (2011). https://doi.org/10.1103/PhysRevLett.106.122004. arXiv:1011.0375 [hep-ph]
12. A. Bzdak, B. Schenke, P. Tribedy, R. Venugopalan, Phys. Rev. C **87**(6), 064906 (2013). https://doi.org/10.1103/PhysRevC.87.064906. arXiv:1304.3403 [nucl-th]
13. P. Bozek, W. Broniowski, Phys. Rev. C **88**(1), 014903 (2013). https://doi.org/10.1103/PhysRevC.88.014903. arXiv:1304.3044 [nucl-th]
14. S.K. Prasad, V. Roy, S. Chattopadhyay, A.K. Chaudhuri, Phys. Rev. C **82**, 024909 (2010). https://doi.org/10.1103/PhysRevC.82.024909. arXiv:0910.4844 [nucl-th]
15. E. Avsar, C. Flensburg, Y. Hatta, J.Y. Ollitrault, T. Ueda, Phys. Lett. B **702**, 394 (2011). https://doi.org/10.1016/j.physletb.2011.07.031. arXiv:1009.5643 [hep-ph]
16. T. Sjöstrand, M. van Zijl, Phys. Rev. D **36**, 2019 (1987). https://doi.org/10.1103/PhysRevD.36.2019
17. I. Bautista, A.F. Téllez, P. Ghosh, Phys. Rev. D **92**(7), 071504 (2015). https://doi.org/10.1103/PhysRevD.92.071504. arXiv:1509.02278 [nucl-th]
18. C. Bierlich, G. Gustafson, L. Lönnblad, A. Tarasov, JHEP **03**, 148 (2015). https://doi.org/10.1007/JHEP03(2015)148. arXiv:1412.6259 [hep-ph]
19. A. Ortiz Velasquez, P. Christiansen, E. Cuautle Flores, I. Maldonado Cervantes, G. Paić, Phys. Rev. Lett. **111**(4), 042001 (2013). https://doi.org/10.1103/PhysRevLett.111.042001. arXiv:1303.6326 [hep-ph]
20. J.R. Christiansen, P.Z. Skands, JHEP **08**, 003 (2015). https://doi.org/10.1007/JHEP08(2015)003. arXiv:1505.01681 [hep-ph]
21. Xr Gou, Fl Shao, Rq Wang, Hh Li, J. Song, Phys. Rev. **D96**(9), 094010 (2017). https://doi.org/10.1103/PhysRevD.96.094010. arXiv:1707.06906 [hep-ph]
22. K.P. Das, R.C. Hwa, Phys. Lett. **68B**, 459 (1977). https://doi.org/10.1016/0370-2693(77)90469-5. [Erratum: Phys. Lett. 73B,504(1978)]
23. R.C. Hwa, Phys. Rev. D **22**, 1593 (1980). https://doi.org/10.1103/PhysRevD.22.1593
24. E. Takasugi, X. Tata, C.B. Chiu, R. Kaul, Phys. Rev. D **20**, 211 (1979). https://doi.org/10.1103/PhysRevD.20.211
25. R.C. Hwa, Phys. Rev. D **51**, 85 (1995). https://doi.org/10.1103/PhysRevD.51.85
26. E. Cuautle, G. Herrera, J. Magnin, Eur. Phys. J. C **2**, 473 (1998). https://doi.org/10.1007/s100520050153. arXiv:hep-ph/9711354 [hep-ph]
27. E. Braaten, Y. Jia, T. Mehen, Phys. Rev. Lett. **89**, 122002 (2002). https://doi.org/10.1103/PhysRevLett.89.122002. arXiv:hep-ph/0205149 [hep-ph]
28. V. Greco, C.M. Ko, R. Rapp, Phys. Lett. B **595**, 202 (2004). https://doi.org/10.1016/j.physletb.2004.06.064. arXiv:nucl-th/0312100 [nucl-th]
29. R.J. Fries, V. Greco, P. Sorensen, Ann. Rev. Nucl. Part. Sci. **58**, 177 (2008). https://doi.org/10.1146/annurev.nucl.58.110707.171134. arXiv:0807.4939 [nucl-th]
30. S. Cao, G.Y. Qin, S.A. Bass, Phys. Rev. C **88**, 044907 (2013). https://doi.org/10.1103/PhysRevC.88.044907. arXiv:1308.0617 [nucl-th]
31. F. Prino, R. Rapp, J. Phys. **G43**(9), 093002 (2016). https://doi.org/10.1088/0954-3899/43/9/093002. arXiv:1603.00529 [nucl-ex]
32. Rq Wang, Fl Shao, J. Song, Qb Xie, Zt Liang, Phys. Rev. **C86**, 054906 (2012). https://doi.org/10.1103/PhysRevC.86.054906. arXiv:1206.4373 [hep-ph]
33. H.h. Li, F.l. Shao, J. Song, R.q. Wang, (2017). arXiv:1712.08921 [hep-ph]
34. J. Song, Xr Gou, Fl Shao, Z.T. Liang, Phys. Lett. **B774**, 516 (2017). https://doi.org/10.1016/j.physletb.2017.10.012. arXiv:1707.03949 [hep-ph]
35. R. Rapp, E.V. Shuryak, Phys. Rev. D **67**, 074036 (2003). https://doi.org/10.1103/PhysRevD.67.074036. arXiv:hep-ph/0301245 [hep-ph]
36. Y. Oh, C.M. Ko, S.H. Lee, S. Yasui, Phys. Rev. C **79**, 044905 (2009). https://doi.org/10.1103/PhysRevC.79.044905. arXiv:0901.1382 [nucl-th]
37. M. Cacciari, M. Greco, P. Nason, JHEP **05**, 007 (1998). https://doi.org/10.1088/1126-6708/1998/05/007. arXiv:hep-ph/9803400 [hep-ph]
38. M. Cacciari, S. Frixione, N. Houdeau, M.L. Mangano, P. Nason, G. Ridolfi, JHEP **10**, 137 (2012). https://doi.org/10.1007/JHEP10(2012)137. arXiv:1205.6344 [hep-ph]
39. J. Adam et al., Phys. Rev. C **94**(5), 054908 (2016). https://doi.org/10.1103/PhysRevC.94.054908. arXiv:1605.07569 [nucl-ex]

40. S. Acharya et al., Eur. Phys. J. C **77**(8), 550 (2017). https://doi.org/10.1140/epjc/s10052-017-5090-4. arXiv:1702.00766 [hep-ex]
41. C. Patrignani et al., Chin. Phys. C **40**(10), 100001 (2016). https://doi.org/10.1088/1674-1137/40/10/100001
42. F. Becattini, U.W. Heinz, Z. Phys. C **76**, 269 (1997). https://doi.org/10.1007/s002880050551. arXiv:hep-ph/9702274 [hep-ph]. [Erratum: Z. Phys. C76,578(1997)]
43. C. Bierlich, J.R. Christiansen, Phys. Rev. D **92**(9), 094010 (2015). https://doi.org/10.1103/PhysRevD.92.094010. arXiv:1507.02091 [hep-ph]
44. M. Bahr et al., Eur. Phys. J. C **58**, 639 (2008). https://doi.org/10.1140/epjc/s10052-008-0798-9. arXiv:0803.0883 [hep-ph]
45. T. Sjöstrand, S. Mrenna, P.Z. Skands, Comput. Phys. Commun. **178**, 852 (2008). https://doi.org/10.1016/j.cpc.2008.01.036. arXiv:0710.3820 [hep-ph]
46. P. Skands, S. Carrazza, J. Rojo, Eur. Phys. J. C **74**(8), 3024 (2014). https://doi.org/10.1140/epjc/s10052-014-3024-y. arXiv:1404.5630 [hep-ph]
47. R. Perez-Marcial, R. Huerta, A. Garcia, M. Avila-Aoki, Phys. Rev. D **40**, 2955 (1989). https://doi.org/10.1103/PhysRevD.44.2203. https://doi.org/10.1103/PhysRevD.40.2955. [Erratum: Phys. Rev. D44,2203(1991)]
48. R.L. Singleton, Phys. Rev. D **43**, 2939 (1991). https://doi.org/10.1103/PhysRevD.43.2939
49. H.Y. Cheng, B. Tseng, Phys. Rev. D **53**, 1457 (1996). https://doi.org/10.1103/PhysRevD.53.1457. https://doi.org/10.1103/PhysRevD.55.1697.2. arXiv:hep-ph/9502391 [hep-ph]. [Erratum: Phys. Rev. D55,1697(1997)]
50. B. Abelev et al., Eur. Phys. J. C **72**, 2183 (2012). https://doi.org/10.1140/epjc/s10052-012-2183-y. arXiv:1208.5717 [hep-ex]
51. S. Acharya et al., Phys. Lett. B **781**, 8 (2018). https://doi.org/10.1016/j.physletb.2018.03.061. arXiv:1712.04242 [hep-ex]